The Simplest Stirred Tank for Laminar Mixing: Mixing in a Vessel Agitated by an Off-Centered Angled Disc

D. Bulnes-Abundis and M. M. Alvarez
Centro de Biotecnología-FEMSA, Escuela de Biotecnología y Alimentos, Tecnológico de Monterrey at Monterrey, Monterrey, NL, C.P. 64849, México

DOI 10.1002/aic.14064
Published online March 14, 2013 in Wiley Online Library (wileyonlinelibrary.com)

We study the mixing structure, mixing performance, and short term dynamics in round bottomed laminar tanks agitated by an eccentrically located angled disc. We define eccentricity ($E = e/R$) as the ratio of the distance of the axis of rotation from the center line of the tank (e) and the tank radius (R). The structural and dynamic features observed at different eccentricity values were compared using planar laser-induced fluorescence techniques and computational fluid dynamics calculations. A Poincaré analysis demonstrates the chaotic nature of the flow induced by eccentricity. Practically globally chaotic conditions are observed for $E = 0.42$ and $E = 0.50$, with mixing times of 5–8 min at $Re = 416$. We study the effect of different injection points on the short-term mixing dynamics and we calculate axial flow rates and Power numbers. Stirred tanks agitated by an eccentrically located angled disc are a simple and cost effective system for laminar mixing applications. © 2013 American Institute of Chemical Engineers *AIChE J*, 59: 3092–3108, 2013
Keywords: mixing structure, mixing time, laminar, eccentric agitation, stirred tank

Introduction

Laminar mixing scenarios are not uncommon in industrial practice. Some relevant examples are the agitation of high-viscosity materials in the food industry[1–3] and in the manufacture of lubricants,[4] the formulation of cosmetics such as creams and unguents, the mixing of liquid detergents, and the agitation of shear-sensitive cells (fungi, plant, insect, and animal cells) in the biopharmaceutical/biotechnology industries.[5–7] In the specific case of biotechnology applications, and particularly in laboratory-scale experiments (for the screening of cell culture conditions, the selection of high-producing clones, or the definition of culture medium, etc.), mixing at low speed is desirable.[7] Nevertheless, stirred tanks are (by far) the most widely used mixing system, even though conventional stirred tank configurations are not well-suited for laminar mixing. Several authors have documented the existence of severe mixing pathologies in conventional laminar stirred tanks.[8–13]

Numerous alternative mixer configurations have been proposed to enhance mixing at low to medium Re numbers, including anchored impellers,[14] coaxial configurations that combine a radial impeller and an anchor impeller,[15] double ribbon impeller configurations,[1] Maxblend® impeller configurations,[16] and other nonconventional geometries that combine impellers that rotate in the same direction[17,18] or in a counter-rotating mode.[18,19] Still others explore novel impeller geometries.[6]

The use of off-centered agitation in laminar stirred tanks has been proposed as a simple strategy to eliminate (or mitigate) laminar mixing pathologies.[11,20,21] Seminal work in eccentric stirred tanks agitated with a horizontal disc (with no blades) or with an axial impeller (four-bladed) in a flat bottom tank was conducted by Alvarez et al. and Sánchez-Cervantes et al.[11,21] The flow structure in these systems was described using planar laser-induced fluorescence (p-LIF) experiments. Although several studies have been recently published on the subject of eccentrically agitated stirred tanks,[21–31] a detailed characterization of mixing and axial flow enhancement in eccentrically agitated laminar tanks is not yet available.

This study analyzes the mixing performance of simple round-bottom stirred tank configurations where agitation is performed by the rotation of an inclined disc impeller (45° with respect to the horizontal plane) in an eccentrically located shaft. Previous work by our group showed that a disc impeller with no blades was capable of producing widespread chaotic conditions in flat bottom stirred tanks in the laminar regime.[21] In this contribution, we introduce two simple, but very significant, geometry modifications (in terms of mixing performance) to previous work[11,21]: we use round-bottomed vessels and angled (45° angle) disc impellers. Different degrees of eccentricity are examined through experimental visualization using p-LIF techniques and computational fluid dynamics (CFD) calculations. The mixing structure and mixing dynamics (including the calculation of mixing times) are studied and compared against those observed in conventional concentrically agitated tank configurations. In addition, we study the short-term dynamics of mixing (during the first minute after a tracer injection) in eccentric systems. In particular, we investigate the effect of selection of the injection point with respect to short-term mixing evolution and initial mixing rates. In the mixing literature, most of the work done so far regarding the effect of injection location in stirred tanks has been focused on

Correspondence concerning author should be addressed to M. M. Alvarez at mario.alvarez@itesm.mx.

blending operations in concentrically agitated systems.[32] In this work, we extend the discussion on the relevance of suitable injection points to eccentrically agitated systems.

Materials and Methods

Experimental stirred tank systems

The stirred tank geometry studied here is a round-bottomed vessel that is agitated using an angled disc impeller (Figures 1a, c, f, g). In this study, flow visualizations and mixing experiments were conducted by positioning the impeller at different eccentricities (indicated in different colors in Figure 1a). Eccentricity (E) was defined as the ratio of the distance between the shaft and the vertical centerline of the tank (e) and the tank radius (R); $E = \frac{e}{R}$. For comparison, flow visualization experiments and/or simulations were also conducted using a horizontal disc impeller (Figure 1b), a concentrically positioned Rushton turbine (Figure 1d) and a concentrically positioned axial HE-3 impeller (Figure 1e). The vessel was immersed in a cubic chamber filled with the same liquid as the tank (not shown) to correct for the optical aberration due to the tank curvature. Drawings in Figure 1f, g indicate the relevant characteristics of the system.

Flow visualization experiments

All visualization experiments reported here were done using glycerin as a model fluid (viscosity approximately equal to 1100 cP at 25°C, measured with a Brookfield DV-E Viscometer). The three-dimensional (3-D) mixing patterns within the bioreactor were revealed using fluorescent tracer injections (Fluorescein, FLUKA, PN:46955) in a dark room where UV light (GE Blacklight F20T12/BL peaking at 370, 440, and 550 nm) was the only illumination source. A better description of the evolution of mixing in time was obtained by conducting p-LIF experiments. In an otherwise dark room, a plane of laser light (Green 532 nm laser; sheet thickness = 1 mm) was directed toward the experimental system, which allowed visual exposure of the mixing structure projected on a vertical 2-D plane originated by the injection of a pulse of fluorescent dye, in this case rhodamine B (Sigma, Catalog number: 83689, USA, absorption spectra peak around 550 nm) dissolved in glycerin. The densities of the dye injection and the bulk of the liquid were matched to minimize buoyancy effects. Tracer injection experiments were conducted at different agitations (200 and 250 revolutions per minute (RPM)) and eccentricity values ($E = 0.0$, $E = 0.13$, $E = 0.30$, $E = 0.42$, $E = 0.50$).

Time series for each experiment were recorded at 3 frames per second (fps) using a professional digital camera (Canon® Rebel XTi). In all cases, the plane inspected (illuminated by the laser sheet) was located ~1 mm behind the impeller shaft. No color filters were used. Images were converted from color to black and white images by applying an appropriate intensity threshold (intensity = 150/255) using free access software (Image J). An in-house image analysis algorithm built in Python® was used to calculate the fraction of the area covered by the dye at each image of each time series. Plots of the evolution of area coverage at different eccentricities and agitation values were constructed based on the analysis of each time series.

CFD vessel geometries

For the CFD simulation, different geometries and their corresponding meshes were created. Figure 1b shows the basic geometry of the vessel used in all simulations. The scheme of the system in Figure 1a shows the location of the impeller at the different eccentricity values used in this work (red $E = 0.0$ (concentric case), blue $E = 0.13$, green $E = 0.42$ and yellow $E = 0.5$). The different impellers used in our CFD studies are shown in Figures 1b–e. To simulate the injection points, four small volumes, designated TIP1, TIP2, TIP3, and TIP4 [after tracer injection point (TIP)], were created in all models. Figure 1b shows the location of these TIPs, color-coded from highest to lowest position: red, blue, green, and yellow, respectively. Figure 1f shows a drawing of the $E = 0.5$ model.

CFD simulations

CFD was used to characterize flow behavior within concentric and eccentric-stirred tank geometries. Computational experiments were done using an HP XW8600® Workstation with two Quad Core Xeon® processors and 16 GB of RAM. Geometries were built using SolidWorks® CAD/CAM Software. Meshing was done via acuMeshsim from Acusim® Software Inc. (Mountview, CA). The resultant models consisted of 500,000 to 1 million nodes and 2–8 million elements (depending on the specific case), with refined mesh near the impeller zone (see also Deglon and Meyer[33]).

The solutions of the velocity fields were calculated using ACUSOLVE from ACUSIM® Software (Mountview, CA). This code was based on a special stabilized Galerkin/least-squares finite element technology formulation of the full nonlinear Navier–Stokes equations. The liquid within the tank was modeled as a Newtonian fluid with the nominal properties of water. ACUSOLVE allows for the transient calculations required to directly describe the complexity of the flow field in eccentric cases, without the need for simplifications or assumptions related to the geometry of the vessel or the way it rotates. In most cases, 60 s of mixing were simulated. Based on the solution of the velocity field for each concentric or eccentric case, different types of results were generated.

Particle tracking was calculated with Acusim AcuTransTrace on this flow. The output from particle tracking was processed with a custom made script[34] to plot particle dispersion in 2-D (Poincare-type sections) and 3-D particle paths in time. Poincaré-type sections were produced by recording the intersection of particle trajectories within a plane positioned at the XY central plane of the tank. For this purpose, 100 particles were located at different TIPs. In addition, particle trajectories in 3-D were followed in time to localize segregated regions and to provide better resolution of the flow structure of the cases studied (concentric and eccentric). Trajectories were generated by releasing 125 particles and by interpolating their location in time based on the velocity field solution. Velocity fields and velocity contours were generated at different horizontal planes to show the 3-D flow structure.

Based on these flow fields, some integral flow properties were calculated; namely, we calculated the integrated volumetric flow rate at different horizontal planes. In addition, a short-term mixing simulation was conducted by releasing 100,000 particles at an initial position and calculating the position of each one of them in a volumetric grid of 100 × 100 × 100 cells. The 3-D coverage of a simulated dye injection can then be estimated by counting the number of cells visited by particle trajectories at any given time. This

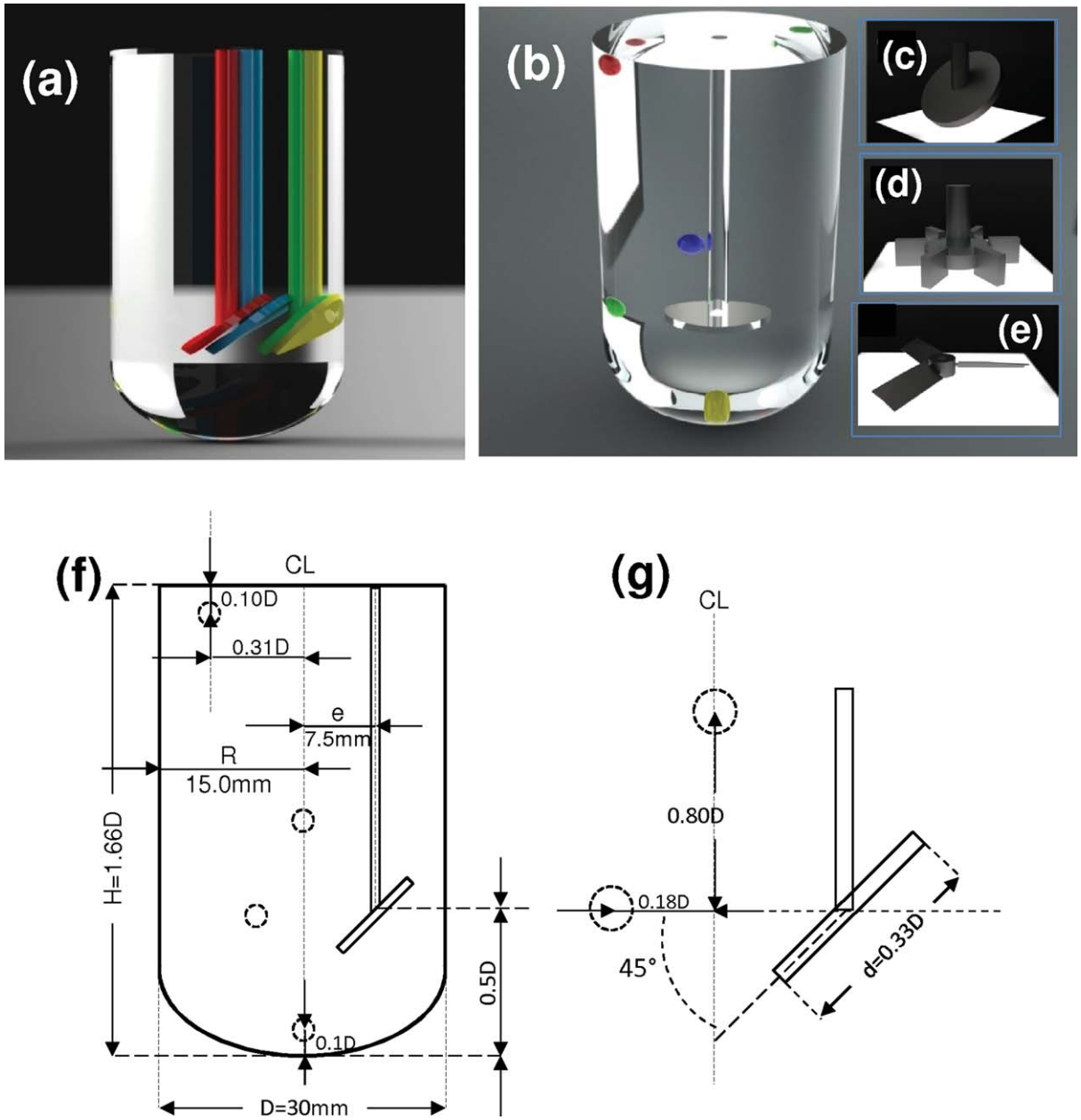

Figure 1. Different stirred tank configurations were studied.

(a) Four different eccentricity values $E = r/R$ were analyzed: $E = 0.0$ (concentric case; red); $E = 0.13$ (blue); $E = 0.42$ (green); $E = 0.50$ (yellow). (b) For comparison, four different concentrically located impellers were used in this work: (b) simple horizontal disc, (c) 45° inclined disc, (d) Rushton 6- blade impeller, (e) HE-3 Hydrofoil impeller. In CFD simulations, four different TIPs were used to release massless fluid particles: TIP1 (red; near the liquid surface); TIP2 (blue; above the impeller plane); TIP3 (green; at the impeller midplane and close to the tank wall); TIP4 (yellow, at the center of the tank bottom). (f) Drawing of a 30-mL vessel with impeller located at $E = 0.5$. Dimensions are in mm. The precise locations of the TIPs are indicated. (g) Details of the impeller geometry.

strategy was used to construct plots of the percentage of the vessel volume covered by a dye injection over time. From these plots, the initial rate of mixing can be calculated by the initial slope of each plot of volume coverage vs. time.

In addition, the Power numbers for eccentric/angled disc configurations and conventional concentrically located impellers (a Rushton turbine and an axial HE-3 propeller) were calculated using CFD. The Power input can be calculated from Eq. 1, where P is the power (P[=] w), N is the RPM value (N [=] rev min^{-1}), and M is the momentum, as calculated from CFD (M[=] $N \cdot m$). The Power number, N_p, was then calculated using Eq. 2, where ρ is the fluid density, N is the RPM value, and D is the impeller diameter

$$P = 2\pi(NM) \tag{1}$$

$$N_P = \frac{P}{\rho N^3 D^5} \tag{2}$$

Results and Discussion

Eccentricity as a strategy to trigger chaos

Chaos leads to mixing in the laminar regime. In general, chaos can be promoted by altering/breaking time or space

symmetries,[20,35,36] causing the structure of the velocity field, and, therefore, the mixing manifolds, to also become asymmetric. The strategy to trigger chaos in a mixing device is system-dependent. In conventional stirred tanks, the mechanism for the creating chaos and the onset of mixing has been studied in detail.[10,20] Briefly, in the laminar regime, conventional concentrically agitated tanks possess a regular flow skeleton.[20,37] This regular flow structure can be understood better if we consider a stirred tank agitated by a concentrically located horizontal disc impeller. This type of system would be a completely axis-symmetric 2-D system,[10,37] where chaos cannot exist unless a periodic perturbation is introduced.[38] Indeed, experimentally, only regular motion is observed in laminar vessels agitated by concentric discs with no blades[37] (Figures 2a, b), and a completely regular structure develops: a series of nested toroidal surfaces. No convective mixing occurs. When an impeller with blades is used, the repetitive (and normally periodic) passing of the blades disturbs the otherwise completely regular flow structure,[10,37] thereby triggering chaos. However, chaos is not widely distributed in concentric laminar stirred tanks. For example, concentrically agitated tanks with one (radial or axial) impeller show isolated toroidal-shaped regions, where regular motion persists (located above and below the impeller), coexisting with two chaotic regions separated by the impeller plane.[8,9,13,35] Even in multiple impeller systems operated in the laminar regime, toroidal structures of regular flow have been observed.[10,12]

Off-centered agitated stirred tanks have been described as an effective alternative for mixing in the laminar regime[11,20–22]. In this case, the mechanism for chaos creation is different; chaos is triggered by disruption of spatial symmetries. In experiments in stirred tanks agitated by horizontal disc impellers located off-center, Alvarez et al.[11] demonstrated that even in the absence of blades, eccentricity generates asymmetric flows and, at some eccentricity values, practically globally chaotic conditions. For example, at $E = 0.42$ (Figures 2c, d), the regular regions observed above and below the impeller plane in a typical concentric system are destroyed.[11] In eccentrically agitated systems, 3-D visualizations (Figure 2c) and Poincaré plots (Figure 2d) reveal a highly convoluted structure. Chaos has been originated by displacement of the axes of rotation. These eccentric systems, consistent in flat bottom tanks agitated by off-centered horizontal disc impellers[11,20,21] were mainly useful as a proof of concept. Although capable of creating practically global chaos, they were not sufficiently efficient and well-suited for practical applications. For example, segregated areas were observed at the corners of the flat bottom. In addition, the flow structure created by a horizontally oriented disk impeller is characterized by a ribbon-like appearance (see Figures 2c, d) that, although it eventually fills the entire space, does it at a lower rate than would other impellers (i.e., axial four-bladed or Rushton impellers) that are capable of producing a sheet-like mixing structure.[10,11]

Indeed, the flow originated by a horizontal disc has a relatively weak axial component when compared to impellers that present more surface area to the fluid. Therefore, conceptually, an inclined disc impeller (see Figure 1c) will be more efficient, in terms of axial pumping, than will a horizontal disc. Indeed, this is the case: when agitation is eccentric with an angled disc impeller, segregation is reduced even further and at a higher rate. In addition, the use of round-bottomed vessels further minimizes the existence of segregated volumes at the tank bottom corners of the vessel (see Figures 2c, d).

Mixing structure at different eccentricities

In this section, we use visualization experiments and CFD simulations to examine in detail the mixing structure and the short-term mixing dynamics originated by eccentric agitation using an angled disk impeller in a round-bottomed tank. Figure 3 shows the development of mixing structure, as revealed by a fluorescent dye injection, in stirred tanks agitated by an inclined disc impeller. The mixing performance of systems with different degrees of eccentricity are compared at low Re values (Re $\sim$ 30, agitation = 300 RPM in glycerin). Glycerin is used as a model fluid to retard the effect of diffusion and allow for a more accurate determination of convective mixing times. In terms of Reynolds values, and consequently mixing structure, these conditions will be approximately equivalent to those observed in water at 0.5 RPM.

Figure 3 shows that the degree of eccentricity determines: (a) the flow structure, (b) the final asymptotic degree of mixing, and (c) the rate of mixing. In the concentric case ($E = 0.0$), after an injection at the surface of the tank, a highly symmetrical structure develops (Figure 3a). The features of the flow reveal the coexistence of chaotic regions of adequate mixing with areas of low-mixing intensity and regular behavior (zones were the fluorescent dye has not yet penetrated). This is consistent with previous reports on stirred tanks operated in the laminar regime, and agitated with Rushton impellers.[8–10,20,35] In addition, the top section of the tank appears to be segregated with respect to the rest of the tank; that is, a zone of poor dye coverage is observed near the liquid surface.

In the eccentric cases, the flow structure becomes progressively asymmetric (Figures 3b, c, d, and e). At $E = 0.13$, the minimum eccentricity tested, the segregated regions in the vicinity of the impeller get distorted but not yet eliminated (Figure 3b), and the flow structure exhibits already certain degree of asymmetry. After 7 min of agitation, a toroidal structure is observable above the impeller plane, although smaller than for the concentric case, and a zone of poor mixing is still evident at the top section of the tank. At $E = 0.30$, the flow becomes fully asymmetric, and the toroidal segregated regions are completely and rapidly eliminated; after only 3 min of agitation, the dye concentration in nearly 50% of the tank is visually homogeneous. However, a vast zone located at the top-distal corner with respect to the impeller does not become integrated into the chaotic region even after 7 min of agitation.

All segregation is practically eliminated at $E = 0.42$ (Figure 3c). At this eccentricity value, the flow appears as globally chaotic, and no regular regions of low mixing persist. The mixing structure develops quickly, and 5 min after the dye injection, practically 90% of the observed tank plane has been covered. In addition, axial circulation was greatly improved with respect the $E = 0.0$, $E = 0.13$, and $E = 0.30$ scenarios. The top region of the tank, which appeared disconnected from the dynamics of the rest of the tank at $E = 0.13$ and $E = 0.30$, looks fully integrated at $E = 0.42$. This is of extreme importance for some practical applications. For instance, in cell culture scenarios, an improved axial circulation enhances oxygen mass transfer from the surface to the bulk of the liquid, which suggests the

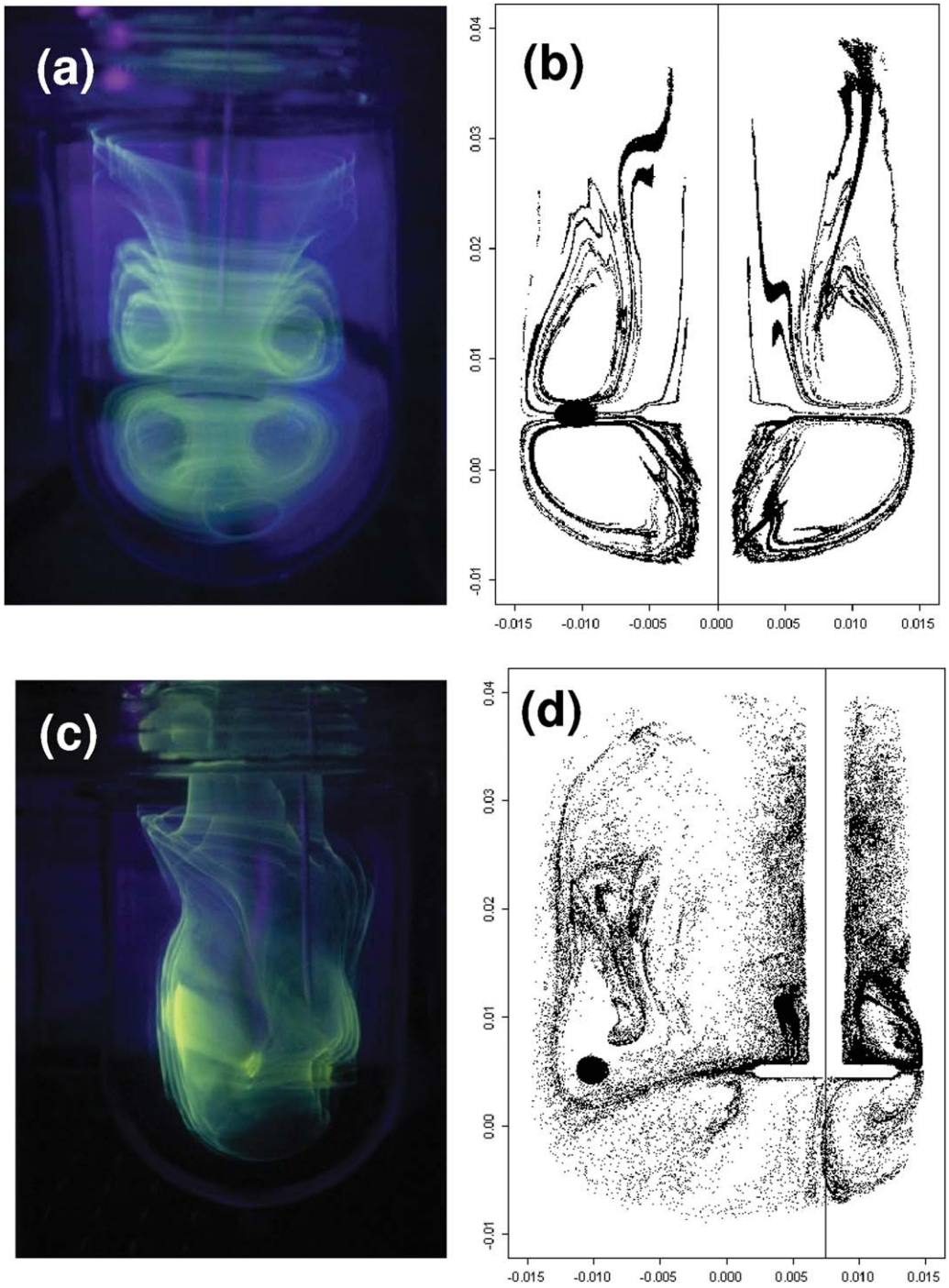

Figure 2. Mixing structure in concentric and eccentric laminar stirred tanks agitated with a flat disc, as revealed by 3-D UV visualizations and Poincaré sections.

(a) 3-D visualization of a tracer injection (fluorescein) in a round-bottom stirred tank agitated with a horizontal disc impeller. (b) The intersection of a blob of particles (initially located at the impeller plane) with the vertical midplane shows a regular structure. (c) 3-D visualizations and (d) Poincaré plots in eccentrically agitated systems.

possibility of use of eccentric agitation to provide adequate oxygenation without resorting to air-sparging. Air-sparging has been described as one of the main causes of lethal cell damage in mammalian cell cultures in stirred tanks.

Globally chaotic conditions are also achieved at $E = 0.47$, and mixing appears to proceed at an even higher rate. Segregation is rapidly destroyed from both the impeller vicinity and the tank surface.

More accurate characterization of the mixing dynamics in these experiments was obtained by recording a series of images and calculating the percentage of area covered by the dye at different times using image analysis algorithms. Figure 4 presents the evolution of the area coverage in time for different eccentricity values, that is, $E = 0.0$, $E = 0.13$, $E = 0.30$, $E = 0.42$, and $E = 0.50$. Mixing proceeds at different rates and reaches different extents (in terms of the total

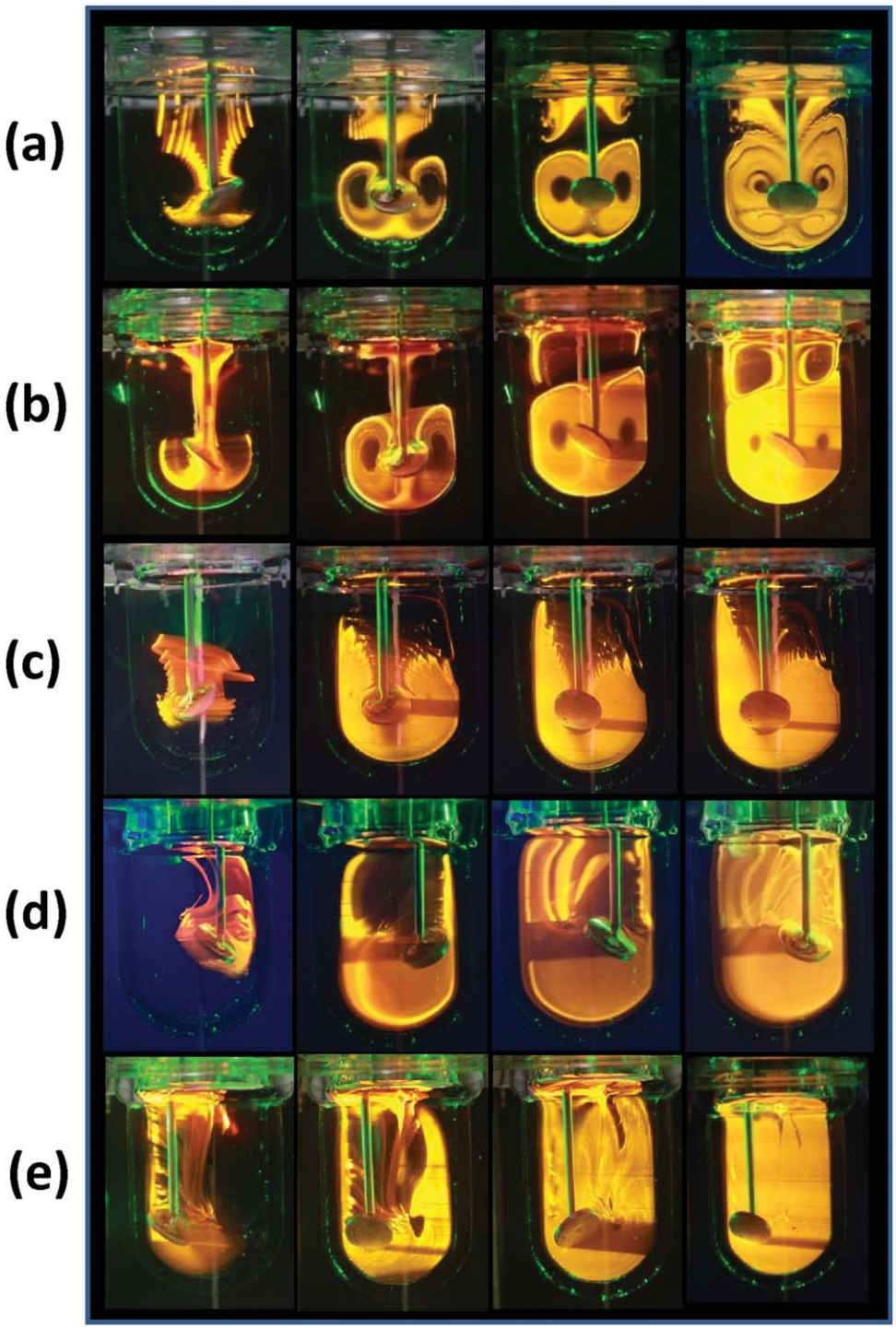

Figure 3. Evolution of the mixing structure after a fluorescent dye injection, as observed in p-LIF experiments, in laminar stirred tanks (Re $\approx$ 4) at different eccentricity values: (a) $E = 0.0$ (a concentric system); (b) $E = 0.13$; (c) $E = 0.30$; (d) $E = 0.42$, and (e) $E = 0.5$ inclined disk.

volume of the system) at different eccentricity values. In this short-term mixing experiment (time frame of less than 10 min) and considering the use of glycerin as a model flow, what is mainly observed are the effects of convective mixing. Note that different eccentricity values produce different values of asymptotic area coverage. For example, in the concentric case ($E = 0.0$), the maximum area coverage asymptotically achieved by convection is $\sim$45–50% after 10 min. In the case of $E = 0.13$, the rate of mixing (the slope of the curve) increases significantly with respect to the concentric case. However, segregation does not disappear completely. The fluorescent dye reveals a mixing structure that covers only 80% of the total area after 1000 s (see also Figures 3a, b). At $E = 0.33$, the mixing rate further improves. Note that the slope of the curve for the case $E = 0.33$ is higher than that corresponding to the case $E = 0.13$ for the first 100 s of the mixing process. However, the mixing structure revealed by the dye injection only fills 56% of the total area. This

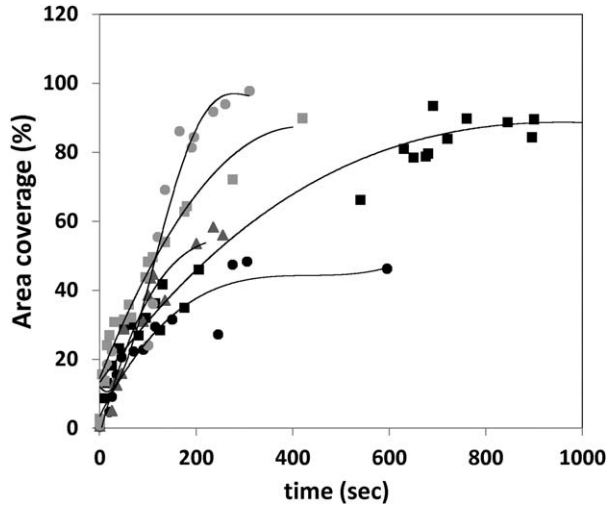

Figure 4. The evolution of the mixing (measured by p-LIF experiments as area coverage at different times) is presented for a tank agitated at 200 rpm by a 45° angled disc located at different eccentricity values: concentrically (•); $E = 0.13$ (■); $E = 0.30$ (▲); $E = 0.42$ (■); and $E = 0.50$ (•).

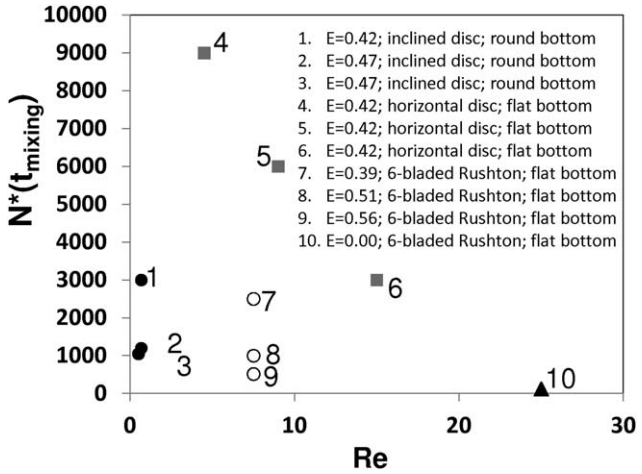

Figure 5. Dimensionless mixing time ($N \times t_{mixing}$) vs. Reynolds number (Re) for different experiments reported in literature (from Sánchez-Cervantes et al., 2006 (■); from Cabaret et al., 2006 (°○) and; from Vallejos et al., 2005 (▲)] or presented in this study (•).

result is somewhat unexpected, because we would intuitively anticipate higher values of dye coverage at higher eccentricity values. At $E = 0.40$ and 0.47, the fluorescent dye eventually covers practically the entire flow domain. However, the rate at which this occurs differs. For this Re value, the process is significantly faster for $E = 0.47$. A mixing $time_{95\%}$ can be defined for the system, since after 5 min of agitation at $Re < 1$ mixing appears 95% complete. Note that this mixing time estimation is only based in a single vertical plane, and, therefore, must be interpreted cautiously. In a conventional concentric geometry, due to the high level of symmetry, all vertical planes will exhibit a similar geometry. In an eccentrically agitated tank, this is not precisely the case, because a very complex 3-D manifold develops. Later in this work, we will discuss and illustrate the advantages of a 3-D mixing time estimation based on CFD calculations. Agitation at $E = 0.42$ also renders a chaotic flow, but with a longer mixing time of ~8 min.

Independently of the asymptotic degree of mixing (or segregation), an initial rate of convective mixing can be formally calculated for each case from the slopes of the linear portion of the curves in Figure 4. Our results suggest that the rate of mixing more than doubles from the concentric case to the eccentric case $E = 0.47$. This is consistent with mixing rate estimations based on CFD calculations that we will present later in this work (see Figure 12).

Eccentricity reduces mixing times

In general, we observed that eccentricity values in the range of $E = 0.40$–0.47 render flows with practically no segregated areas (globally chaotic flows) with mixing $times_{95\%}$ in the order of 6–8 min at $Re < 1$ (points #1,2, and 3 in Figure 5). An obvious question is how mixing times in this eccentric/inclined disc configuration compare with those reported in other laminar mixing studies In Figure 5, we present in the same 2-D space data (Re vs. dimensionless mixing time) from Vallejos et al.[39] (2005), Cabaret et al.,[26] and this study. Mixing times in the laminar regime ($Re < 50$) and at different eccentricities were reported by Alvarez[20] and Alvarez et al.[21] for flat-bottomed vessels agitated by eccentrically located disc impellers and four-bladed axial impellers. In those studies, mixing times on the order of 10 min were calculated by LIF for eccentric systems, with $E = 0.42$. More recently, Sánchez-Cervantes et al.[21] discussed the effect of the diameter of a disc impeller on mixing time in flat bottom eccentric tanks in the laminar regime ($Re < 30$). The authors estimated relatively short-mixing times (on the order of 5–6 min) for a stirred tank with a 1000-mL volume agitated with a 3-cm diameter horizontally oriented disc at 500 rpm ($Re \approx 15$; point #6 in Figure 5). Similarly, in experiments performed in the laminar regime ($Re = 1.5$–13.0; using a radial impeller), Cabaret et al.[26] reported the occurrence of practically complete mixing (as evaluated by a similar technique), only in the narrow window of eccentricity values from $E > 0.257$ to $E > 0.56$ and $7.5 < Re < 13.0$. Indeed, for the lowest Re value where complete mixing was observed ($Re = 7.5$), E values in the range of $E = 0.39$ to $E = 0.56$ were required (points #7, 8, and 9 in Figure 5). The use of eccentricity, a round bottom, and an inclined disc impeller achieves practically complete mixing at the lowest Re values (in comparison with other impeller and tank configurations). Lower dimensionless mixing times are achievable using other configurations (eccentric radial impellers, as in Cabaret et al.,[26] or a concentric radial impeller, as in Vallejos et al.,[39] at much higher relative Re values. This suggests that the stirring configuration studied here would provide adequate mixing in laminar vessels at lower RPM values (and consequently lower tip speed values) than other configurations. This can be very useful in the context of culture of shear-sensitive cells, such as CHO cells, stem cells, plant cells, and fungus broths (see also Bulnes-Abundis et al., 2012).[7] In practice, this also implies adequate mixing at lower power input and shear stress. Later in this article, we will present and discuss shear stress and Power number calculations for concentric and eccentric stirred tanks.

Analysis of structural features using CFD

A more robust analysis of the mixing features in stirred tanks was conducted using CFD techniques. CFD is now commonly used to simulate flow behavior in conventional and newly proposed stirred tank geometries.[9,12,32,33] The CFD simulations make what-if scenarios easier to study. In addition, CFD simulations help to overcome some of the intrinsic errors associated with injection or velocimetry experiments in stirred tanks (e.g., slight variations in shaft or impeller position among runs, tracer injection volume, rate of injection, density or viscosity differences of the tracer solution, etc.). For example, using CFD calculations, we can obtain more accurate estimates of the distribution of chaotic and regular zones in a concentric or eccentric flow (if a flow is truly globally chaotic).

In concentrically agitated systems, even globally chaotic flows exhibit a great deal of heterogeneity.[36,40,41] In stirred tanks and other partially or globally chaotic flow systems, the distribution of properties, such as the intermaterial area

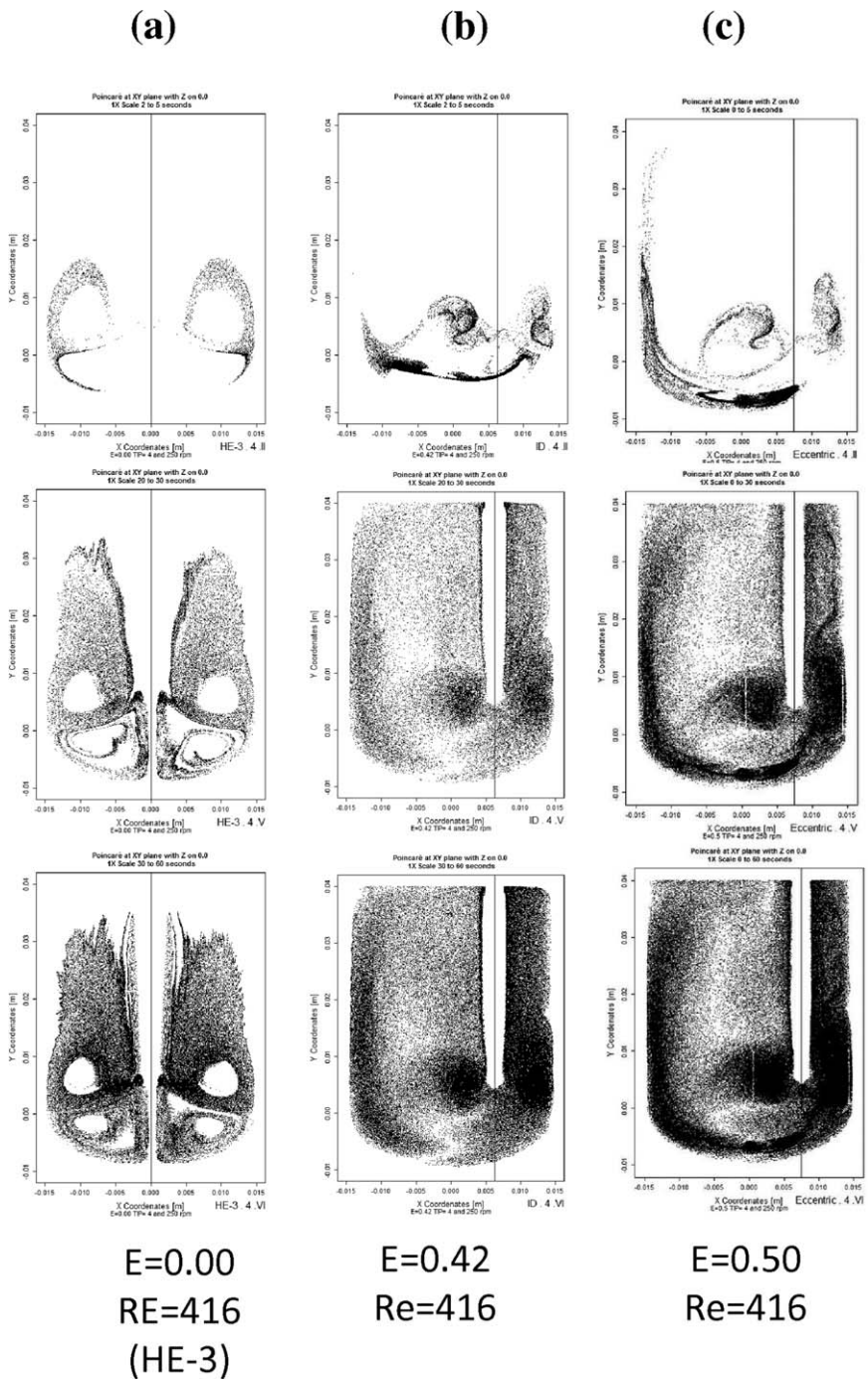

Figure 6. Poincaré sections originated by 60 s of laminar flow in stirred tanks (Re = 416) agitated by (a) a concentrically located HE-3 impeller; and eccentrically located angled disks at (b) $E = 0.42$, and (c) $E = 0.50$.

The intersection of the trajectories of 10,000 particle originated at TIP3 with the vertical midplane were recorded at three different time intervals: from 2 to 5 s after injection (first row); from 20 to 30 s after injection (second row); and from 30 to 60 s after injection (third row).

density[40,41] and the stretching, span more than five orders of magnitude.[12] Figure 6 presents Poincaré-type sections for flows in stirred tanks agitated by inclined impellers at different eccentricity values ($E = 0.42$; $E = 0.5$), and for a concentric system agitated with a conventional HE-3 axial impeller. In each simulation, 100 particles are liberated in an initial location (tracer injection point 4; TIP4 see Figure 1) and followed for 60 s. The time interval from 2 to 5 s, 20 to 30 s, and 30 to 60 s are shown. Each time that a particle crosses the tank, vertical midplane a point is recorded. Therefore, these Poincaré maps reveal the areas of the flow that are effectively being visited in a particular plane of the flow. Because the point of injection was selected in the chaotic region of the tank, regular isolated regions will appear as being deprived of particles. Regions of high visitation will appear as more densely covered. For the concentric case, the Poincaré plots reveal the coexistence of chaos and order (Figure 6a).

As previously observed for other axial and radial impellers, regular regions above and below the impeller are evident. Although a densely visited region is present at the impeller vicinity, a vast area of the middle plane (~50%) has not been crossed by particle trajectories after 1 min of mixing. In particularly, the upper tank region remains poorly explored. In contrast, tanks agitated with an angled, eccentrically located disc impeller, for the same time frame and Reynolds number, show Poincaré sections that indicate widespread chaos and an evident difference in the mixing rate can be observed when the Poincaré maps corresponding to the first 20 s of agitation are compared (Figures 6a, b, c).

A nonsymmetrical dispersion pattern emerges as time progresses. From 20 to 30 s, practically the entire flow domain has been explored by chaotic trajectories (except for a small region at the upper-left corner of the tank). Note that the frequency of visitation is higher in some areas of the tank, whereas some others appear less densely crossed. However, in terms of visitation frequency, the relatively small displacement of the impeller shaft from the center line (13%) has practically eliminated segregation and caused a more homogeneous visitation frequency distribution. For $\mathrm{Re} = 416$, at $E = 0.42$ and $E = 0.50$, practically globally chaotic conditions are achieved. During an agitation period of 30 s, the entire flow domain has been visited.

Short-term mixing dynamics at different injection locations

In many practical applications, a liquid material must be injected into a stirred tank already in operation. Illustratively, during typical bioprocesses, the metabolism of microorganisms induces a migration of the pH from a set point (more commonly an acidification). Concentrated acid or base solutions are added to the system to control pH. In these cases, rapid mixing is desirable for proper distribution of the injected material in the least time possible, to minimize gradients of concentration, which can diminish product yield or affect growth or other metabolic indicators of the microorganism in use. In reactive systems, the practical relevance of selecting an adequate injection point for reactants, particularly in the context of fast chemical reactions, has been widely recognized.[32,42,43] Indeed, the idea is well-accepted that in a reactive stirred tank system, an adequate selection of an injection location results in minimization of secondary reactions, and, therefore, a maximization of product yield.

In this section, we investigate whether the injection location matters in terms of short-term mixing dynamics in eccentrically agitated reactors. Concentric stirred tank configurations are well-known to show the fastest short-term dispersion when the injection point is at the impeller discharge.[44] Reports on the short-term dynamics of mixing at different TIPs in eccentrically agitated vessels are not available. As illustrated before, the flow structure, and, therefore, the mixing topology, of eccentrically agitated systems is far more complicated than that of concentrically agitated ones. Indeed, it is not intuitive to predict, *a priori*, the flow skeleton in an eccentric system. It is precisely the flow skeleton, the manifold of the flow, which determines the fate of any tracer injected into the system. Therefore, a detailed calculation of this manifold is required for a precise diagnosis of the effectiveness of an injection point. CFD studies can provide that description. Studies of short-term evolution/dispersion of tracer injections, composed of multiple particles, allow comparisons of the rate and extent of mixing at different injection points.

For illustration purposes, we took the best mixing eccentric scenario ($E = 0.42$), according to the analysis of mixing structures and mixing times previously presented, and computationally performed injection tracer experiments at four different tank locations (see Figures 1b and 7). Regardless of the TIP, eccentric flows rapidly disperse the particles and practically the same mixing structure is observed 60 s after injection. In eccentrically agitated tanks, injection location is only important during a very short-time period. In Figure 7, differences are observed between different columns (different TIPs) during the first 20 s of the dispersion process. After 30 s of agitation, all dispersion plots, regardless of the point of injection, look essentially identical. These findings suggest that eccentrically agitated stirred tanks that exhibit globally chaotic conditions (i.e., $\mathrm{Re} = 416$ and $E = 0.42$,) disperse material in a very efficient manner, such that "the memory" of the point of injection fades quickly (in less than 30 s). Counterintuitively, our results suggest that, at higher eccentricity values (i.e., $E = 0.50$), some differences are evident between injection points in the very short term. After 60 min of agitation, the mixing rate appears to be higher for TIP3. At higher Re numbers ($\mathrm{Re} = 4166$) and $E = 0.50$, the result of the dispersion process is practically identical for TIP2, TIP3, and TIP4. However, for TIP1, located at the vicinity of the liquid surface, the dispersion process still appears delayed (Figure 8).

Similar experiments performed in concentric tanks agitated by Rushton turbines (data not presented) reveal that the effect of different TIPs lasts much longer. In some particular cases, for example, for injections at the liquid surface (a very common injection point for pH control), differences in dispersion plots with respect to TIPs at the impeller discharge are notorious for more than 1.5 min (for $\mathrm{Re} = 416$). In more extreme cases, for example, at lower Re numbers and when the TIP is located within a segregated toroidal region of regular motion, the material injected remains trapped indefinitely (see Figure 9).

CFD experiments reveal 3-D features of concentric and eccentric flows

Conclusions derived about mixing performance based on the exclusive inspection of only one vertical plane (in this case the tank midplane) can be misleading. This cautionary

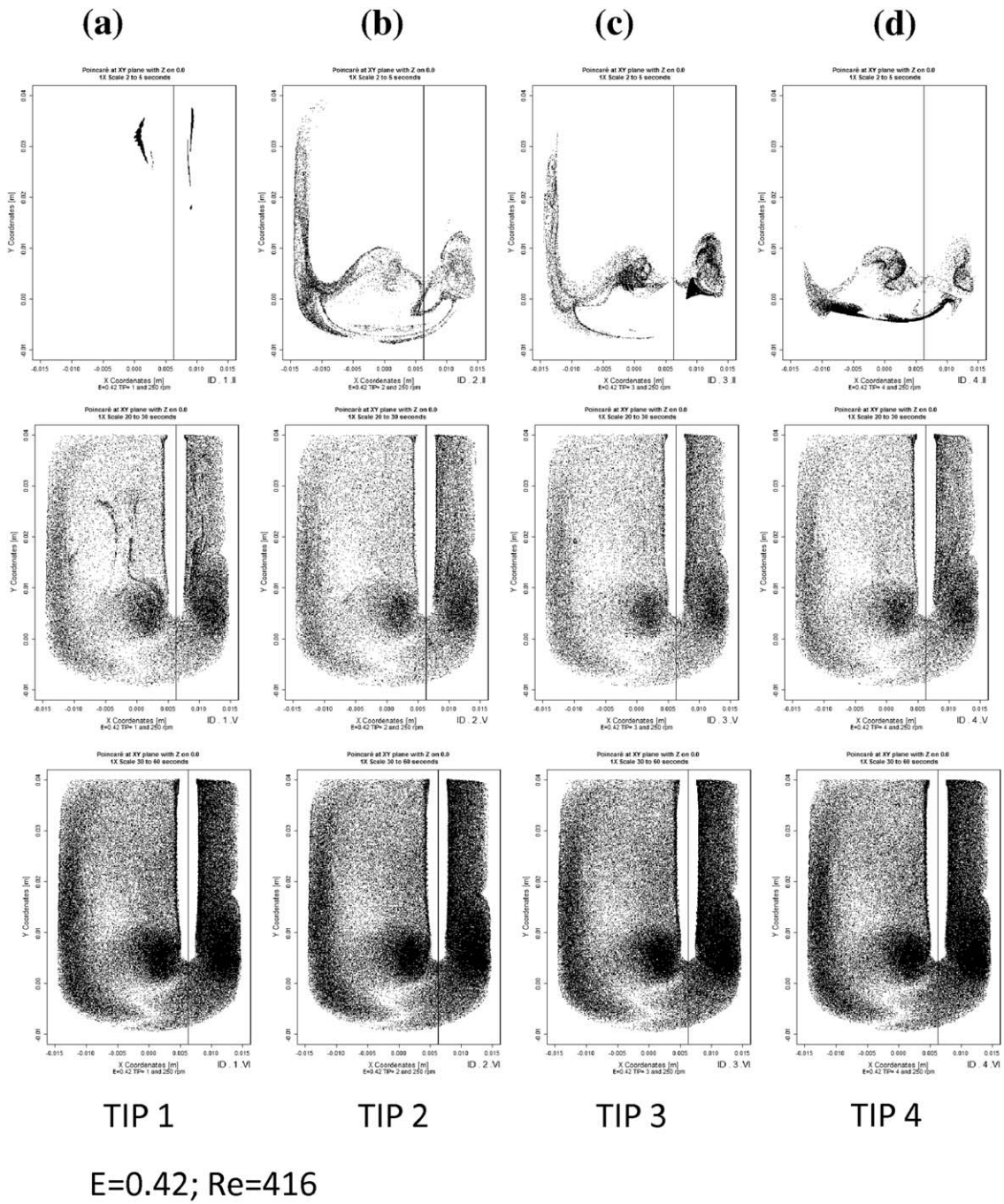

Figure 7. Poincaré sections originated by 60 s of laminar flow in stirred tanks (Re = 416) agitated by an eccentrically located angled disk at $E = 0.42$.

The dispersion of a tracer injection composed by 10,000 particles was originated from four different tracer injection positions: (a) TIP1, (b) TIP2, (c) TIP3, and (d) TIP4. The intersections of each one of the particle trajectories with the vertical midplane are recorded at three different time intervals: from 2 to 5 s after injection (first row); from 20 to 30 s after injection (second row); and from 30 to 60 s after injection (third row).

statement is particularly valid in the case of the highly convoluted 3-D flows induced by eccentrically located impellers. In this section, we use CFD to characterize short-term mixing in concentric and eccentric stirred tank configurations. In particular, we demonstrate that, by displacing the agitation shaft off center ($0.40 < E > 0.47$), we effectively address two mixing pathologies typically observed in laminar and transitional stirred tanks: the separatrix at the impeller midplane[13] and the toroidal segregated regions observed above and below the impeller.[8,35]

Concentric laminar tanks agitated with typical axial[11], or radial impellers[13,26] cause an extremely impermeable separation plane that seriously obstructs the circulation between the top and the bottom portion of the tank, practically converting the top and bottom sections in independent reactors from the convective point of view.[12,13,21] In Figure 9a, we follow the 3-D trajectory of group of particles initially seeded above (Figure 9a) and below (Figure 9b) the impeller plane of a round-bottomed tank agitated (Re = 416) by a concentrically located Rushton impeller. Note that the trajectories of

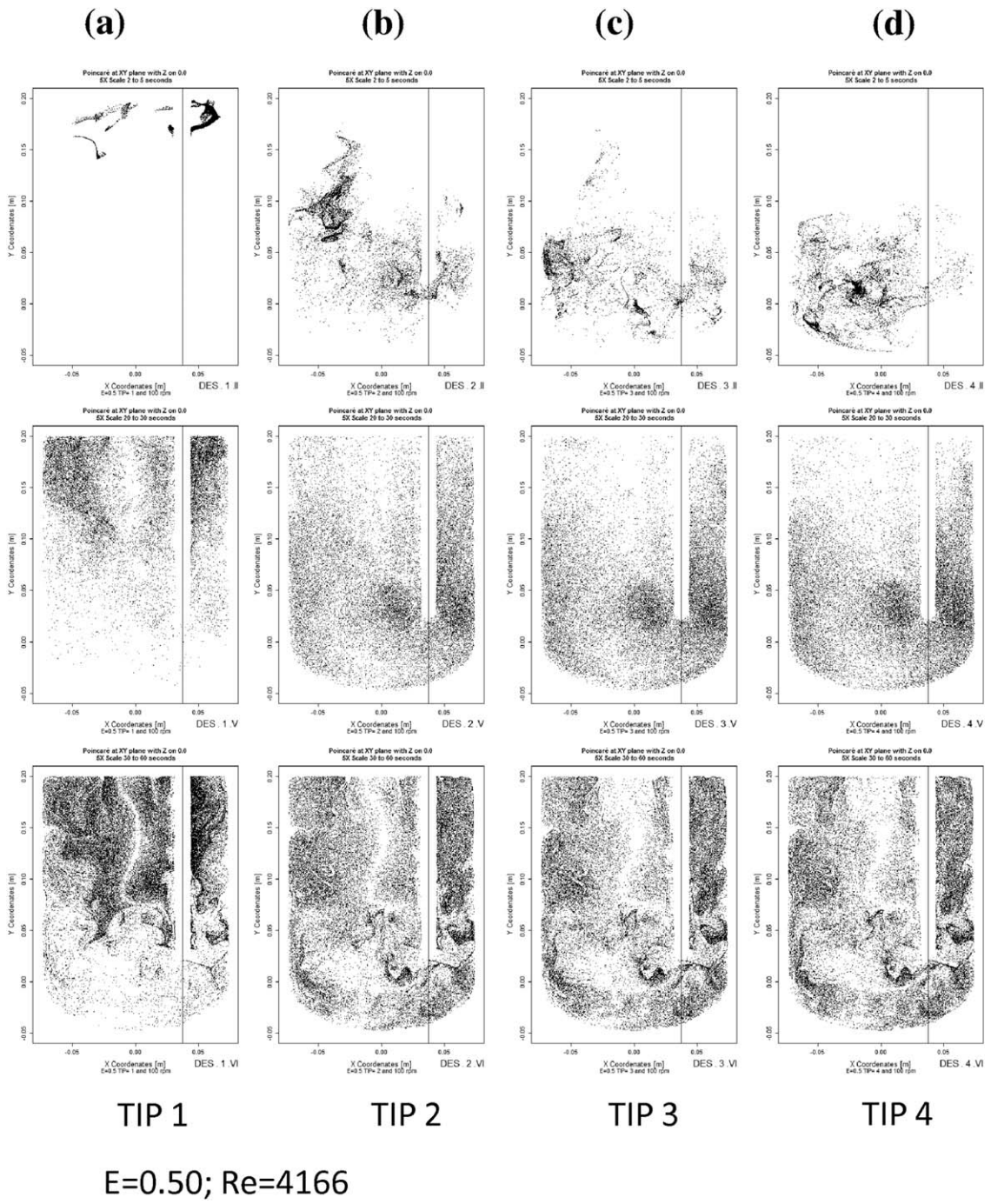

Figure 8. Poincaré sections originated by 60 s of transitional flow in stirred tanks (Re = 4166) agitated by an eccentrically located angled disk at $E = 0.50$.

The dispersion of a tracer injection composed by 10,000 particles was originated from four different tracer injection positions: (a) TIP1, (b) TIP2, (c) TIP3, and (d) TIP4. The intersections of each one of the particle trajectories with the vertical midplane are recorded at three different time intervals: from 2 to 5 s after injection (first row); from 20 to 30 s after injection (second row); and from 30 to 60 s after injection (third row).

particles initially located in the upper section of the tank do not explore the lower region delimited by the impeller plane. Similarly, the trajectories corresponding to particles initially injected in the bottom section do not visit the upper region.

In Figure 9d, 125 particle tracers are located in each of four initial conditions (coded with different colors) in a round-bottomed tank agitated by a concentrically located Rushton turbine. Particles initially seeded inside the toroidal segregated regions remain trapped within them during the entire time of this simulation (yellow and blue trajectories) and the impeller plane acts as an impermeable separatrix. Particles initially seeded in the chaotic region above the impeller do not cross the impeller plane. Similarly, particles injected into the chaotic region below the impeller plane do not explore the upper section of the tank. In a more realistic, conventional concentric reactor, the presence of sensors, baffles, sampling devices, or bubbling would introduce asymmetries and perturbations to this basic flow field and would

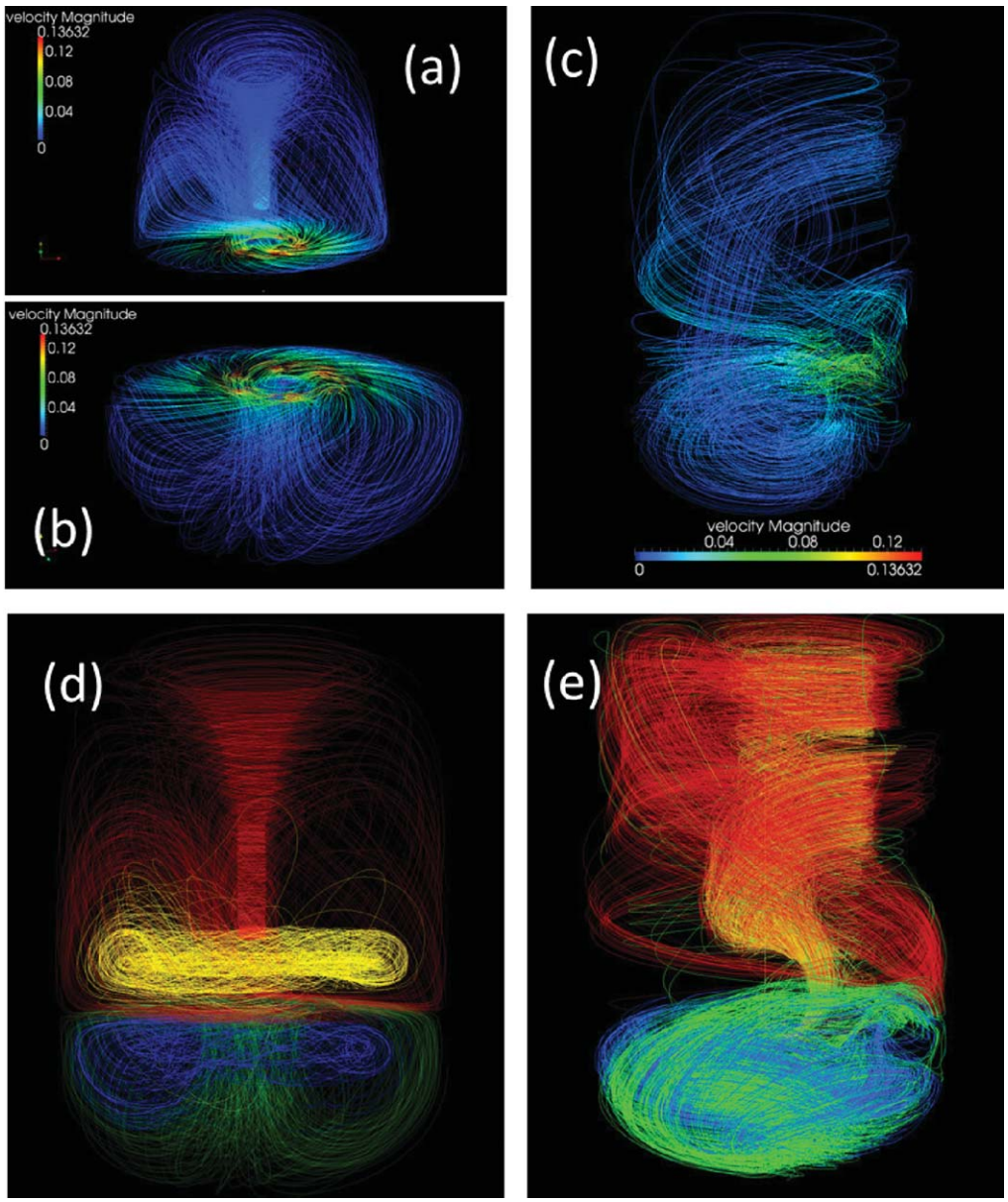

Figure 9. CFD calculations of 3-D particle trajectories in concentrically and eccentrically agitated stirred tanks.

(a) Trajectories of 25 particle tracers initially located above the impeller plane of a tank agitated at 250 RPM (Re = 416) by a conventional Rushton impeller located concentrically, (b) trajectories of 25 particle tracers initially located below the impeller plane of a tank agitated at 250 RPM (Re = 416) by a conventional Rushton impeller located concentrically, and (c) trajectories of 25 particles initially seeded below the impeller plane of a tank agitated by a 45° angled disc impeller located eccentrically ($E = 0.42$) at Re = 416. Trajectories have been color coded accordingly to local velocity magnitudes. In addition, (d) shows the streamlines drawn by the trajectories described by 100 massless tracer particles for 7.2 s within a round-bottom tank concentrically agitated by an inclined impeller. Particles were seeded at different locations: (yellow particles in the upper toroidal segregated region; blue particles in the lower toroidal segregated region; green particles in the chaotic region bellow the impeller; and red particles in the chaotic region above the impeller). (e) Particle trajectories produced by an eccentrically agitated impeller [same initial locations and speed as in (d)].

promote some top-bottom mixing. As shown in previous studies,[13] even in those cases, the impeller separation plane should be considered as an important obstacle to axial circulation in concentric stirred tanks.

In Figure 9e, the CFD simulation experiment is repeated for a tank agitated by an inclined disc impeller eccentrically positioned. After only 7.2 s of agitation, the fluid particles seeded in the upper tank section already explore the bottom region. Similarly, the particles seeded at the bottom of the tank now explore the uppermost region of the tank. Not only the impeller separation plane, but also the segregated toroidal regions above and below the impeller plane,[8–10] are destroyed by eccentricity ($E = 0.42$) at low Re values ($N = 250$ RPM in water; Re $\approx$ 416). Other differential features can be observed between concentric and eccentric tank configurations. In the concentric case (see Figure 9a), particle trajectories in the lower compartment are projected from the impeller discharge, to the tank walls, to later descend near the walls until they converge at the center of the tank bottom. Consequently, solid particles (for example cells) tend to be driven to the deepest point of the tank.

The ascending local velocities that prevail at these locations are low and some solid particle deposition is expected in this zone. In contrast, the flow structure at the bottom of an eccentric system sweeps the tank surface with circulatory trajectories and, as observed in Figure 9b, the center of the circulatory pattern at the tank bottom is not located at the deepest point of the tank. Conceptually, this fact and the circulatory motion at the bottom minimize the problem of particle settlement and potentially reduce the just suspension velocity required for a particular particle size and density.

Top circulation is also significantly improved in eccentric systems. Results presented in Figures 9c, e provide evidence of the improvement of axial circulation near the gas-liquid interface in eccentric systems. For the same RPM values, the frequency of trajectory visitation to the fluid surface is higher in eccentric systems (compare Figures 9d, e).

Axial flow enhancement in eccentric systems

As stated before, conventionally stirred tanks are usually agitated by radial impellers (Rushton turbines) or axial propellers (diverse models are in use: the hydrofoil impeller, elephant ears, Ekhato models, HE-3 from Chemineer, etc). In the mixing literature, the idea is well-accepted that axial impellers promote better axial mixing (top-bottom circulation). Despite this fact, most industrially relevant applications rely on Rushton turbines.

Different ways are available to evaluate axial circulation in stirred vessels. Frequently, 2-D flow velocity fields are used to illustrate the magnitude of the axial circulation. Here, a different approach is used. The construction of velocity isosurfaces using CFD allow the visualization of flow structures. The more convoluted isosurface suggests a more complex flow structure. Figure 10 contrasts the flow structure, as revealed by an isosurface of constant local velocity of 0.02 m/s, of different impeller configurations studied here. On the isosurface, different colors indicate the magnitude value of the y-velocity component. This simple visualization strategy allows examining the 3-D flow in the vicinity of the impeller, providing visual information about the axial pumping capacity of the impeller in use. In the case of the Rushton turbine, this zone is completely symmetrical and does not expand further that a few millimeters away from the impeller (Figure 10a). In all inclined disc/eccentric cases (Figures 10b–d), the volume described by the isosurface is more convoluted and significantly asymmetrical.

A more direct comparison of the axial pumping capabilities of different impeller configurations was obtained by integrating the axial flow (flow rate in the y-direction) over circular 2-D planes at different heights of the tank (Figure 11). In this plot, the color scale indicates both intensity and direction. Surprisingly, in terms of axial flow, the concentric Rushton and the eccentric/angled impeller configurations clearly outperform the HE-3 system, an impeller specifically designed for superior axial pumping. In general, the concentric Rushton system

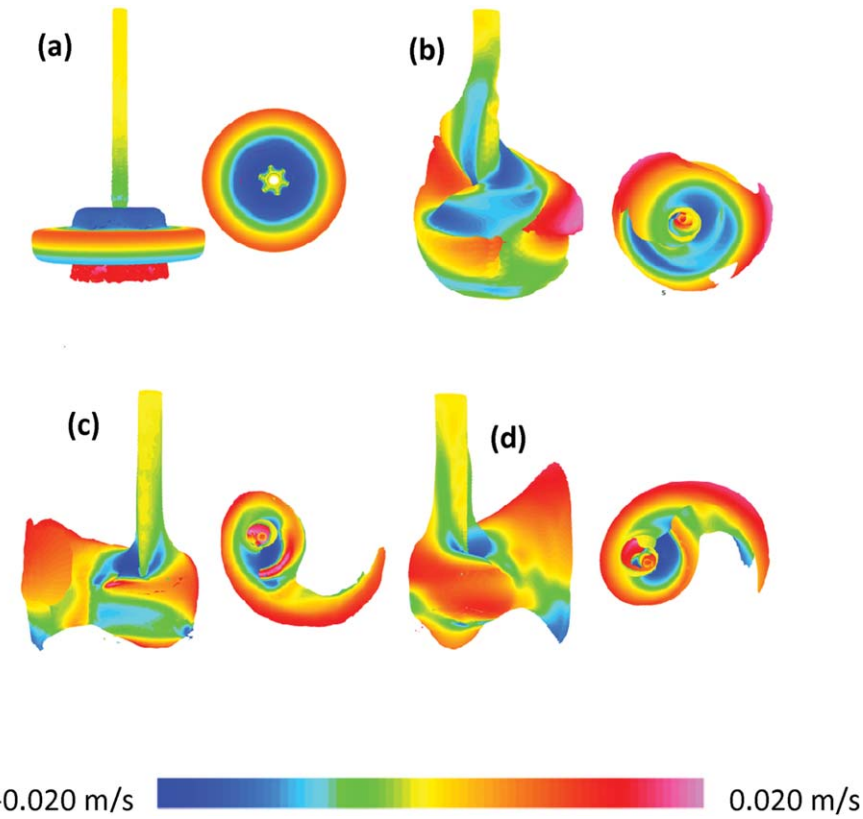

Figure 10. Isosurfaces of velocity magnitude = 0.02 m/s in different stirred tank configurations calculated by CFD simulations: (a) the isosurface created by the flow originated by a Rushton impeller, (b) an angled disk at $E = 0.13$, (c) an angled disk at $E = 0.42$, and (d) an angled disk at $E = 0.5$.

The axial component of the flow was indicated by coloring the isosurfaces based on the vertical component of the velocity field (y-velocity). For all configurations, stirring speed was set at 250 RPM (Re = 416).

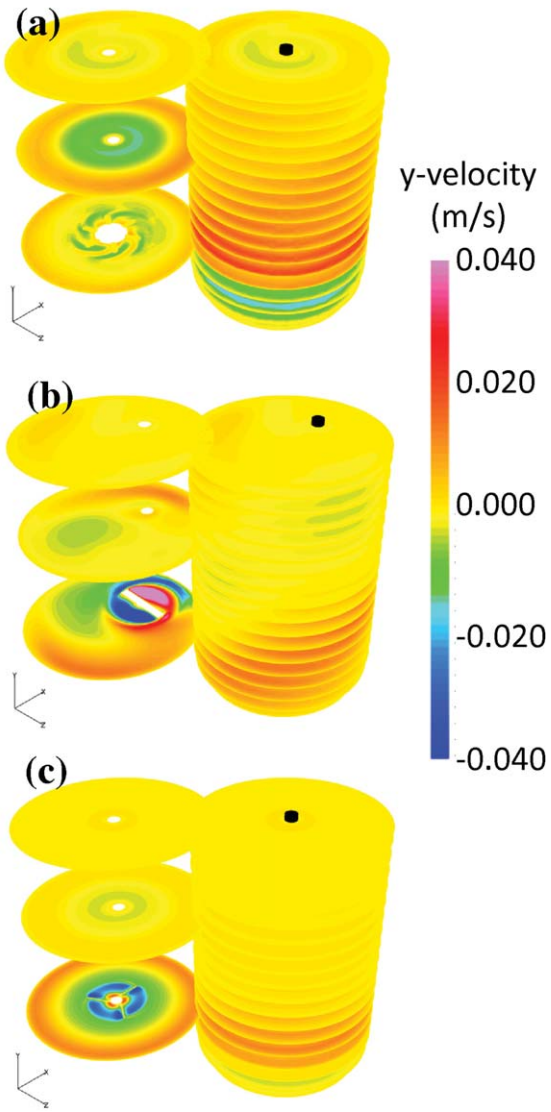

Figure 11. Calculation of the flow rate per unit of area [based on c(CFD) simulations] at different vertical planes in stirred tanks agitated by (a) a concentrically located Rushton impeller; (b) an eccentrically located ($E = 0.42$) angled disc impeller; and (c) a concentrically located HE-3 impeller.

originates areas of higher flow rates (upward and downward) than the eccentric/angle disc. These areas of high upward and downwards flow are symmetrical, concentric, and highly localized. This denotes a highly heterogeneous (in terms of flow intensities) but cyclic (or periodic) flow structure. In the eccentric/angled configuration, the asymmetric distribution of the areas of up and down circulation and the smoothness of the flow field suggests a more complex flow structure and a more evenly distributed axial circulation.

Estimation of 3-D mixing rates using CFD

The experimental investigation of mixing, mixing times, and flow structure through dye injections is intrinsically affected by the very same act of intruding the system to perform the injection. Besides, in real dye injection experiments (such as those presented previously), it is only possible to retard, but not eliminate, the effects of diffusion (diffusive mixing).

At present, computational estimations of purely convective mixing rates (and conceptually even mixing times) are possible using CFD. Figure 12 shows the 3-D mixing evolution calculations based on the simulation of the convective transport of a dye injection. A set of points (1 million) was liberated at the different TIPs (TIP1, TIP2, TIP3, and TIP4). The entire 3-D flow domain was divided into 1×10^5 boxes. The number of boxes in the tank volume visited by at least one of these particles was calculated. In Figure 12, the evolution of the percentage of boxes visited with respect to time for the first 60 s of agitation is plotted for eccentric/angled disc configurations, and concentric Rushton and HE-3 systems. From the slope of the linear portion of each volume coverage vs. time plot, the initial rate of mixing can be calculated. In the case of eccentrically agitated systems, for the same Re value, the rate of mixing is practically the same for different TIPs (Figure 12a). In contrast, in concentrically agitated systems, regardless of the axial or radial nature of the flow, the initial rate of mixing is highly dependent on the initial point of injection (Figures 12b, c). For instance, for the case of systems agitated by a Rushton turbine, dramatic differences are seen in mixing rates if the injection occurs in TIP1 or TIP3. Interestingly, although the best injection point for the Rushton system is TIP3, the best injection locations for the HE-3 system are TIP2 and TIP4 (see also Varley and Birch; and Bujalski et al.).[32,44]

Figure 12d compares the initial mixing rates (slopes from the curves presented) for different systems. Tanks agitated by eccentrically located angled discs clearly outperform concentrically stirred systems. Interestingly, eccentric systems ($E = 0.42$ and $E = 0.50$) exhibit a sustained constant mixing rate over time during the first 60 s of agitation. This is not the case for concentrically agitated vessels. For instance, in concentric Rushton configurations injected at TIP3, the initial rate of mixing was comparable to that observed in eccentric systems. However, this high value was not sustained during the first 60 s of agitation. Among eccentrically agitated systems, tanks at $E = 0.42$ exhibit higher initial mixing rates than tanks at $E = 0.50$.

The calculation of mixing rates based on CFD has some limitations. For example, the grid resolution, the time resolution, and the number of particles in the initial injection have to be decided arbitrarily. These parameters might have an effect on the calculated absolute value of the volume fraction visited. However, if the same set of parameters is maintained for all simulations under study, for the same Re and agitation time, results should allow a comparative evaluation of mixing performance.

The cost of good mixing in eccentric systems

We have discussed the advantages of using eccentrically located angle disc impellers in stirred tanks. One valid concern is the cost, in terms of power input, of the observed mixing improvement. Using CFD, we calculated the Power number for different impeller configurations (eccentrically located angled disc impellers, and Rushton turbines and HE-3 axial impellers concentrically located) in a wide range of

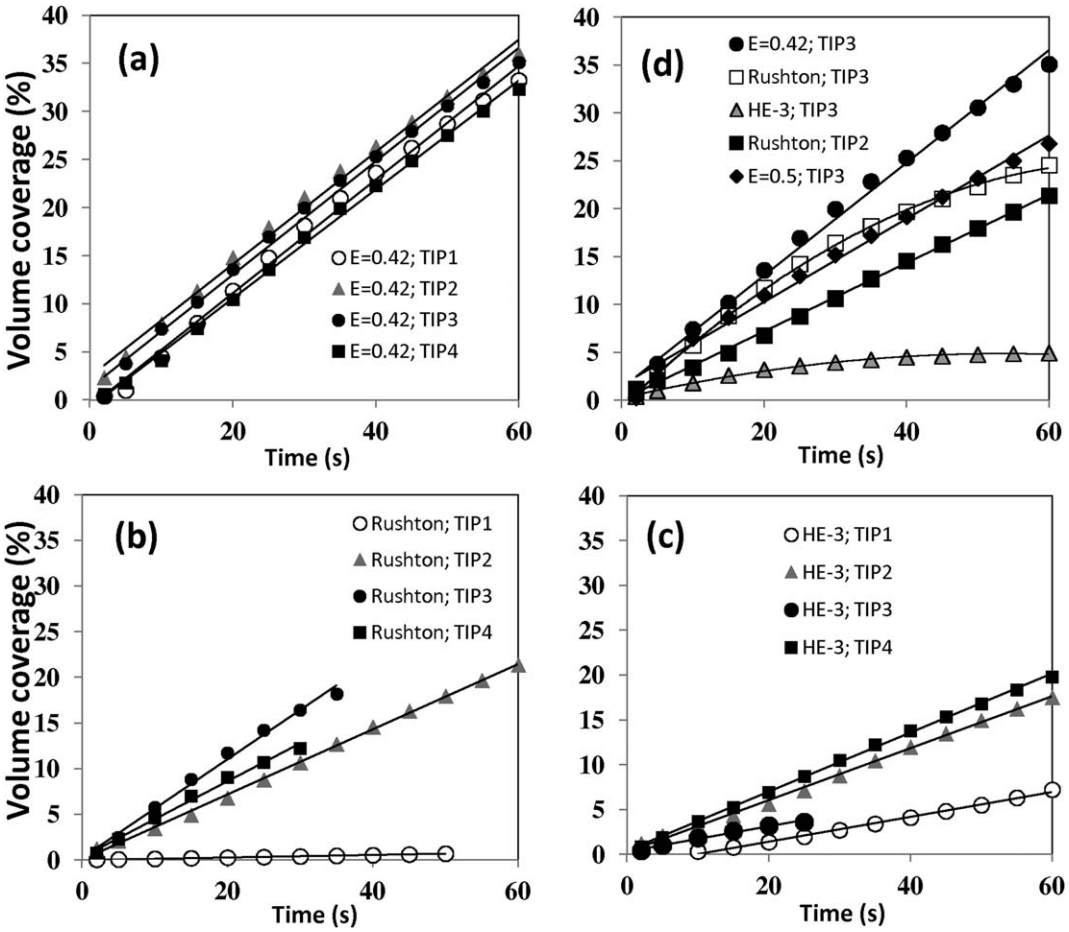

Figure 12. Evolution of the volume coverage of a tracer, as calculated by CFD simulations, during the first 60 s after injection of a tracer in different stirred tank configurations: (a) an eccentric system ($E = 0.42$) agitated with an angled disc impeller and initially injected at different TIPs; (b) a concentric system agitated by a Rushton turbine initially injected at different TIPs; and (c) a concentric system agitated by a HE-3 axial impeller initially injected at different TIPs; (d) comparison of the evolution of the volume coverage during the first 60 s of agitation in different tank configurations.

Reynolds numbers in the laminar and transitional regime (Figure 13). Our calculations for conventional concentric impellers (Rushton and HE-3 impellers) are consistent with data in literature,[45–47] which provides validation for the algorithm of our calculation. Results suggest that in terms of Power number, and regardless of the eccentricity value, angled disc impellers behave similarly to concentrically located Rushton turbines in the low laminar regime. As shown before, in the low laminar regime ($Re < 500$), the mixing performance of eccentric/angled disc configurations is far superior to that of concentric Rushton systems.

In the range of $Re > 500$, the Power number in eccentric impellers is higher than in Rushton turbines. Concentrically located axial HE-3 impellers are more economical than eccentric configurations in terms of Power number for the same Re value, but, as shown before, also exhibit lower mixing performance in the range of $Re < 500$. Power number values reported for other mixing configurations (such as helicon ribbons and coaxially arranged anchor and Rushton turbines) are higher than those calculated for angled/eccentric configurations in the laminar regime (Foucault et al., 2005; Fradette et al., 2007).[15,19] Our results suggest that eccentric stirred tank systems exhibit adequate axial dispersion characteristics at moderate power input.

Conclusions

In this study, we have characterized the mixing and flow dynamics of a simple stirred tank configuration capable of cost effective mixing in the laminar and transitional regime. Three features are relevant in the design of this mixing vessel: (1) rounded bottom; (2) use of an inclined disc impeller; and (3) eccentricity of the impeller shaft. From these three elements, eccentricity is the most determinant, and defines a chaotic flow structure. Previous reports have shown that an effective way to disrupt flow symmetry in a stirred tank is by moving the agitation shaft to an off-centered position. Here, we demonstrate that angled disc impellers can further improve mixing performance in eccentrically agitated rounded bottom tanks. Experimental mixing times in eccentric systems were considerably shorter than in concentric tanks agitated by radial or axial impellers. We also calculated initial rates of mixing for concentric and eccentric systems for different injection points using CFD. We found that

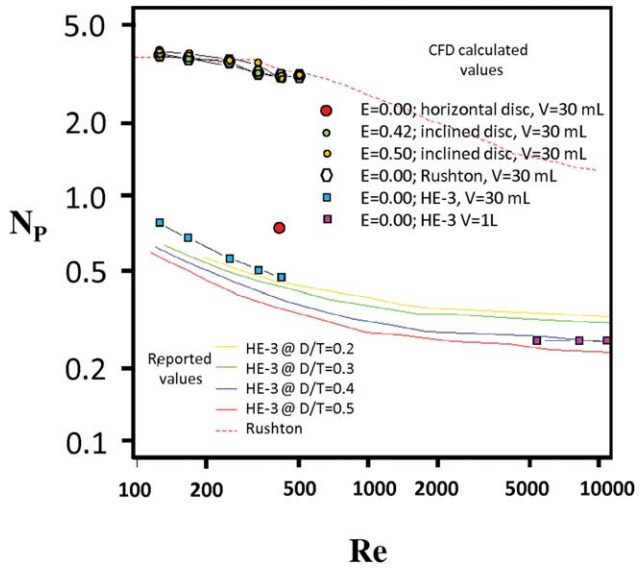

Figure 13. Plot of Power Number vs. Re for different tank-impeller configurations.

For reference, curves of Power Number vs. Re for conventional concentric impeller configurations are presented: HE-3 at D/T = 0.2 (yellow line); HE-3 at D/T = 0.3 (green line); HE-3 at D/T = 0.4 (blue line); HE-3 at D/T = 0.5 (continuous red line); Rushton impeller (dotted red line).

initial mixing rates are higher in eccentric configurations and, in contrast with concentrically agitated vessels, are not dependent on the initial point of injection. Our results suggest that eccentric stirred tank configurations can be an adequate solution for one important and classic laminar mixing problem: effective mixing in highly viscous environments using remarkably simple impeller geometry at a reasonable power input.

Acknowledgments

The authors acknowledge the financial support provided by the Mexican government through CONACYT scholarships for DBA. The authors are grateful for the financial support provided by Tecnológico de Monterrey at Monterrey through Cátedra de Investigación (CAT 122).

Literature Cited

1. Maingonnat JF, Doublier JL, Lefebvre J, Delaplace G. Power consumption of a double ribbon impeller with Newtonian and shear thinning fluids and during the gelation of an iota-carrageenan solution. *J Food Eng*. 2008;87(1):82–90.
2. Bouvier L, Moreau A, Line A, Faqtah N, Delaplace G. Damage in agitated vessels of large visco-elastic particles dispersed in a highly viscous fluid. *J Food Sci*. 2010;76(5):E384–E391.
3. Migliori M, Correra S. Modelling of dough formation process and structure evolution during farinograph test. *Int J Food Sci Technol*. 2012;48(1):121–127.
4. Franco JM, Delgado MA, Valencia C, Sánchez MC, Gallegos C. Mixing rheometry for studying the manufacture of lubricating greases. *Chem Eng Sci*. 2005;60 (8–9):2409–2418.
5. Dusting J, Sheridan J, Hourigan K. A Fluid dynamics approach to bioreactor design for cell and tissue culture. *Biotechnol Bioeng*. 2006;94(6):1196–1208.
6. Lin Y, Thibault J. Pullulan fermentation using a prototype rotational reciprocating plate impeller. *Bioprocess Biosyst Eng*. DOi: 10.1007/s00449-012-0816-z.
7. Bulnes-Abundis D, Carrillo-Cocom LM, Aráiz-Hernández D, García-Ulloa A, Granados-Pastor M, Sánchez-Arreola PB, Murugappan G. Alvarez MM. A simple eccentric stirred tank mini-bioreactor: mixing characterization and mammalian cell culture experiments. *Biotechnol Bioeng*. 2013;110(4):1106–1118. doi: 10.1002/bit.24780.
8. Lamberto DJ, Álvarez MM, Muzzio FJ. Experimental and computational investigation of the laminar flow structure in a stirred tank. *Chem Eng Sci*. 1999;54:919–942.
9. Lamberto DJ, Alvarez MM, Muzzio FJ. Computational analysis of regular and chaotic mixing in a stirred tank reactor. *Chem Eng Sci*. 2001;56(16):4887–4899.
10. Alvarez MM, Zalc JM, Shinbrot T, Arratia PE, Muzzio FJ. Mechanisms of mixing and creation of structure in laminar stirred tanks. *AIChE J*. 2002;48(10):2135–2148.
11. Alvarez MM, Arratia PE, Muzzio FJ. Laminar mixing in eccentric stirred tank systems. *Can J Chem Eng*. 2002;80(4):546–557.
12. Zalc JM, Szalai ES, Alvarez MM, Muzzio FJ. Using CFD to understand chaotic mixing in laminar stirred tanks. *AIChE J*. 2002;48(10):2124–2134.
13. Alvarez MM, Guzmán A, Elías M. Experimental visualization of mixing pathologies in laminar stirred tank bioreactors. *Chem Eng Sci*. 2005;60(8-9 SPEC. ISS.):2449–2457.
14. Pedrosa SMCP, Duarte CG, Nunhez JR. Improving the flow of stirred vessels with anchor type impellers. *Comput Aided Chem Eng*. 2000;8(C):403–408.
15. Foucault S, Ascanio G, Tanguy PA. Power Characteristics in coaxial mixing: Newtonian and non-Newtonian fluids *Ind Eng Chem Res*. 2005;44:5036–5043.
16. Hidalgo-Millán A, Zenit R, Palacios C. On the hydrodynamics characterization of the straight Maxblend® impeller with Newtonian fluids. *Chem Eng Res Design*. 2012;90(9):1117–1128.
17. Hidalgo-Millán A, Taboada B, Vega-Alvarado L, Zenit R, Ascanio G. Enhancement of laminar mixing in stirred vessel using geometrical perturbations. *J Appl Res Technol*. 2012;10(4):520–533.
18. Wang X, Fradette L, Takenaka K, Tanguy P. Effect of operating parameters on the mixing performance of the superblend coaxial mixer. *Ind Eng Chem Res*. 2012;51(4):1826–1833.
19. Fradette L, Thomé G, Tanguy PA, Takenaka K. Power and mixing time study involving a Maxblend® impeller with viscous Newtonian and non-Newtonian fluids. *Chem Eng Res Design*. 2007;85(11A):1514–1523.
20. Álvarez MM. Using spatiotemporal asymmetry to enhance mixing in chaotic flows: from maps to stirred tanks. Ph. D. Thesis, Chemical and Biochemical Engineering. Rutgers University, New Brunswick, NJ, 2000.
21. Sánchez-Cervantes MI, Lacombe J, Muzzio FJ, Alvarez MM. Novel bioreactor design for the culture of suspended mammalian cells. Part 1: mixing characterization. *Chem Eng Sci*. 2006;61(24):8075–8084.
22. Ascanio G, Brito-Bazán M, Brito-de La Fuente E, Carreau PJ, Tanguy PA. Unconventional configuration studies to improve mixing times in stirred tanks. *Can J Chem Eng* 2002;80(4):558–565.
23. Karcz J, Cudak M, Szoplik J. Stirring of a liquid in a stirred tank with an eccentrically located impeller. *Chem Eng Sci*. 2005;60(8-9):2369–2380.
24. Montante G, Bakker A, Paglianti A, Magelli F. Effect of the shaft eccentricity on the hydrodynamics of unbaffled stirred tanks. *Chem Eng Sci*. 2006;61(9):2807–2814.
25. Szoplik J, Karcz J. Mixing time of a non-Newtonian liquid in an unbaffled agitated vessel with an eccentric propeller. *Chem Pap*. 2008;62(1):70–77.
26. Cabaret F, Fradette L, Tanguy PA. Effect of shaft eccentricity on the laminar mixing performance of a radial impeller. *Can J Chem Eng*. 2008;86(6):971–977.
27. Galleti CH, Brunazzi E. On the main flow features and instabilities in an unbaffled vessel agitated with an eccentrically located impeller. *Chem Eng Sci*. 2008;63(18):4494–4505.
28. Yang FL, Zhou SJ, Zhang CX, Chen LF. Investigation on solid-liquid suspension performance in an eccentrically stirred tank. *Guochengg Gongcheng Xuebao/Chinese J Process Eng*. 2008;8(6):1064–1069.
29. Yang FL, Zhou SJ, Wang GC. Experimental study and detached eddy simulation of the macroinstability in an eccentric stirred tank. *Appl Mechan Mater*. 2011;66–68:20–26.

30. Woziwodzki S, Jedrzejczak Ł. Effect of eccentricity on laminar mixing in vessel stirred by double turbine impellers. *Chem Eng Res Design*. 2011;89(11):2268–2278.
31. Takahashi K, Shigihara D, Takahata Y. Laminar mixing in eccentric stirred tank with different bottom. *J Chem Eng Jpn*. 2011;44 (12):931–935.
32. Bujalski JM, Jaworski Z, Bujalski W, Nienow AW. The influence of the addition position of a tracer on CFD simulated mixing times in a vessel agitated by a Rushton turbine. *Chem Eng Res Design*. 2002;80 (8):824–831.
33. Deglon DA, Meyer CJ. CFD modelling of stirred tanks: numerical considerations. *Miner Eng*. 2006;19(10):1059–1068.
34. Bulnes-Abundis D. CFD as a tool for the characterization of mixing performance, shear stress distributions and adequacy for cell culture of stirred tanks agitated by eccentrically located inclined disks. Ph.D. Thesis. Tecnológico de Monterrey, Monterrey, México, 2012.
35. Lamberto DJ, Muzzio FJ, Swanson PD, Tonkovich AL. Using time-dependent RPM to enhance mixing in stirred vessels. *Chem Eng Sci*. 1996;51(5):733–741.
36. Hobbs DM, Alvarez MM, Muzzio FJ. Mixing in globally chaotic flows: a self-similar process. *Fractals*. 1997;5(3):395–425.
37. Alvarez-Hernández MM, Shinbrot T, Zalc JM, Muzzio FJ. Practical chaotic mixing. *Chem Eng Sci*. 2002;57(17):3749–3753.
38. Ottino J. *The kinematics of mixing: stretching, chaos and transport* (1st edition). Cambridge University Press, 1989.
39. Vallejos JR, Kostov Y, Ram A, French JA, Marten MR, Rao G. Optical analysis of liquid mixing in a bioreactor. *Biotechnol Bioeng*. 2005;93(5):906–911.
40. Alvarez MM, Muzzio FJ, Cerbelli S, Adrover A, Giona M. Self-similar spatiotemporal structure of intermaterial boundaries in chaotic flows. *Phys Rev Lett*. 1998;81(16):3395–3398.
41. Muzzio FJ, Alvarez MM, Cerbelli S, Giona M, Adrover A. The intermaterial area density generated by time- and spatially periodic 2D chaotic flows. *Chem Eng Sci*. 2000;55(8):1497–1508.
42. Kling K, Mewes D. Two-colour laser induced fluorescence for the quantification of micro- and macromixing in stirred vessels. *Chem Eng Sci*. 2004;59(7):1523–1528.
43. Hu Y, Wang W, Shao T, Yang J, Cheng Y. Visualization of reactive and non-reactive mixing processes in a stirred tank using planar laser induced fluorescence (PLIF) technique. *Chem Eng Res Design*. 2012;90 (4):524–533.
44. Varley J, Birch J. Reactor design for large scale suspension animal cell culture. *Cytotechnology*. 1999;29(3):177–205.
45. Bates RL, Fondy PL, Corpstein RR. An examination of some geometrical parameters of impeller power. *Ind Eng Chem Proc*. 1963;2:310–314.
46. Hemrajani RR, Tatterson GB. Mechanically stirred vessels. In: Paul EL, Atiemo-Obeng VA, Kresta SM, editors. Handbook of Industrial Mixing: Science and Practice. New Jersey: John Wiley and Sons, Inc., 2004:345–389.
47. Yapici K, Karasozen B, Schäfer M, Uludag Y. Numerical investigation of the effect of the Rushton type turbine design factors on agitated tank flow characteristics. *Chem Eng Process Process Intensif*. 2008;47(8):1340–1349.

Manuscript received Oct. 11, 2012, and revision received Jan. 8, 2013.